

Cite this: DOI: 00.0000/xxxxxxxxxx

Received Date
Accepted Date

DOI: 00.0000/xxxxxxxxxx

Mixing–Demixing Transition in Polymer-Grafted Spherical Nanoparticles

Peter Yatsyshin,^{*a} Nikolaos G. Fytas,^{*b} and Panagiotis E. Theodorakis^{*c}

Polymer-grafted nanoparticles (PGNPs) can provide property profiles that cannot be obtained individually by polymers or nanoparticles (NPs). Here, we have studied the mixing–demixing transition of symmetric copolymer melts of polymer-grafted spherical nanoparticles by means of coarse-grained molecular dynamics simulation and a theoretical mean-field model. We find that a larger size of NPs leads to higher stability for given number of grafted chains and chain length reaching a point where demixing is not possible. Most importantly, the increase in the number of grafted chains, N_g , can initially favour the phase separation of PGNPs, but further increase can lead to more difficult demixing. The reason is the increasing impact of an effective core that forms as the grafting density of the tethered polymer chains around the NPs increases. The range and exact values of N_g where this change in behaviour takes place depends on the NP size and the chain length of the grafted polymer chains. Our study elucidates the phase behaviour of PGNPs and in particular the influence of the grafting density on the phase behaviour of the systems anticipating that it will open new doors in the understanding of these systems with implications in materials science and medicine.

1 Introduction

Inorganic nanoparticles (NPs) dispersed in polymer hosts have attracted much attention over the last decades in multiple technological areas, such as electronics, medicine, and others^{1–3}. In these applications, nanocomposite materials have property profiles that cannot be obtained by using polymers or NPs alone, for example, NPs in a polymer host must avoid aggregation. However, creating homogeneous mixtures of NPs and polymers turns out to be challenging, due to the attractive van der Waals forces between NPs and the polymer-mediated depletion interactions^{4,5}. A possible solution to this problem is NPs grafted with polymer chains^{6–10}, known as polymer-grafted or polymer-tethered NPs (PGNPs), which can be self-suspended with homogeneous particle dispersion in the absence of any solvent^{11–15}. Density functional theory has indicated that the phase stability is due to the space-filling constraint on the grafted corona chains^{13,16,17}, which leads to an effective attraction of entropic origin between NPs, which is also mediated by the attached polymer chains. In this case, the Flory–Huggins parameter may be larger and more negative^{17,18}. Another reason for the steric stabilization of the NPs may be the absence of the solvent and the presence of incompressible poly-

mer chains. This results in the suppression of long wavelength fluctuations that induces an effective attraction between the particles^{13,16–19}. The constraints on the corona imposed by space-filling have been in the centre of attention of recent work, and in particular, the dependence on the core particle size^{12–15,20}, chain length^{13,14,21,22}, grafting density^{2,12,13,21,23–25}, and temperature^{2,12,26}. Recently, there has been also studies of PGNPs in blends with chemically distinct polymers focusing on the physical properties, structure, and underlying dynamics of these systems¹¹. This latter work has been corroborated with theoretical results that allowed the estimation of the heat of mixing of the PGNP blends as a function of the volume fraction of the system¹¹.

A theoretical description of the phase behaviour for PGNPs mixtures based on arguments of the Flory–Huggins theory^{27,28} is challenging, even for the most symmetric cases in composition and molecular architecture. This is due to the fact that the theoretical assumptions related to a necessary effective χ_{eff} parameter that describes systems of PGNPs require extensive testing and validation with experimental and simulation results. This effective parameter would correspond to an effective chain length N_{eff} of effective polymer chains, $\chi_{\text{eff}} \sim N_{\text{eff}}$. Moreover, $\chi = \alpha/T + \beta$, where α and β are parameters for the enthalpic and entropic contributions to χ ²⁹. These parameters are controlled by the interaction between the different components. In addition, the interplay between entropic and enthalpic contributions is affected in a nontrivial manner by parameters pertaining to the architecture of PGNPs. As a result, the theoretical prediction of χ for these

^a Department of Chemical Engineering, Imperial College London, South Kensington Campus, SW7 2AZ London, UK; E-mail: p.yatsyshin@imperial.ac.uk

^b Applied Mathematics Research Centre, Coventry University, Coventry CV1 5FB, United Kingdom; E-mail: nikolaos.fytas@coventry.ac.uk

^c Institute of Physics, Polish Academy of Sciences, Al. Lotników 32/46, 02-668 Warsaw, Poland; E-mail: panos@ifpan.edu.pl

systems is far from being under command.

In this work, we address this issue by studying the order-disorder transition (ODT) of composition- and molecular-symmetric spherical PGNP melts, *i.e.*, the attached polymer chains are all of the same length, NPs are spherical and of the same size and the same grafting density, but grafted polymer chains differ in their chemical type. The symmetry of our system will allow us to isolate main features that dictate the phase behaviour of PGNPs. By using molecular dynamics (MD) simulations of a bead-spring model^{12,30–32}, we demonstrate that the variation of the NPs size leads to higher stability of the melts for given grafting density and length of the polymer chains. For small and intermediate size of NPs we find a transition region that reflects a change in the phase behaviour of the system. Initially, the increase in the number of grafted chains favours the separation of the PGNPs. However, further increase renders the demixing of PGNPs more difficult for a given polymer length and NP size. One possible explanation of this behaviour is the increase of the effective core size of PGNPs that is due to the increase in the number of the tethered chains around the spherical core particle. The range and location of this change in behaviour depends on the NP size and chain length. A simple understanding of these findings can be gained in terms of an intuitive mean-field model, where the PGNP melt is coarse-grained as a fluid mixture, with components having repulsive interactions. Overall, our results describe the mixing/demixing tendencies of symmetric PGNPs melts elucidating the specific effects of PGNPs core, which are at the heart of the PGNPs molecular architecture for moderate size of NPs and grafted polymer chains. In this way, we anticipate that our findings will provide a fundamental understanding towards the design of PGNPs structures, which is important for advanced applications in materials science, medicine, and beyond.

2 Methodology

We implemented MD simulations of a standard bead-spring model in the NPT ensemble by using the large-scale atomic/molecular massively parallel simulator (LAMMPS)³³. The pressure and temperature of the system was fluctuating around predefined values during the course of the simulation. In our case, the temperature was $T = 0.8\epsilon/k_B$ with ϵ being the unit of energy and k_B the Boltzmann constant, while the pressure ($P = 0.1\epsilon/\sigma^3$, where σ is the unit of length) corresponded to the ambient pressure and is the value used in previous studies^{12–15}. Each simulated PGNPs copolymer melt consists of 500 molecules placed in a cubic simulation box with periodic boundary conditions applied in all Cartesian directions. Each molecule is composed of a spherical core particle with diameter, D , which are labelled in our model with the index 'c'. Here, we have considered the cases $D = 1\sigma, 4\sigma$, and 7σ , which are suitable for our simulations^{12–15}. Linear polymer chains of either type A or B monomers are grafted to each core NP with grafting density $d_g = N_g/A_c$, where $A_c = \pi D^2$ is the surface area of the core particle in units of σ^2 , and N_g is the number of grafted chains. The number of grafted chains, which is the same for all PGNPs in the melt, in this study ranges from 5 to 40 when $D = 4\sigma$ or 7σ , while for $D = 1\sigma$ the maximum number of grafted chains is $N_g = 15$,

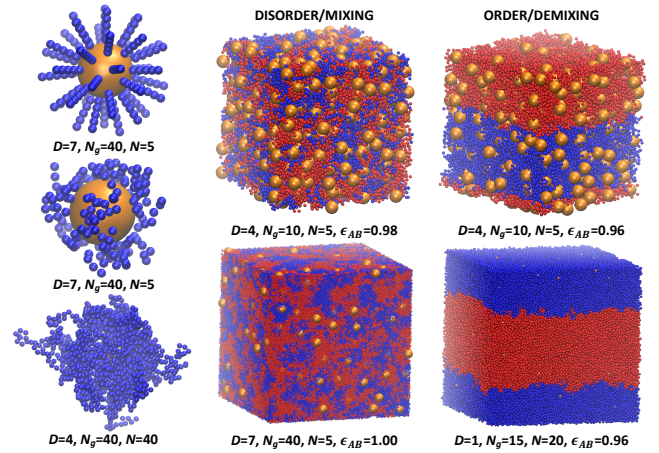


Fig. 1 Left panel from top to bottom depicts the molecular architecture of a PGNP, which is used to construct the initial configuration of the system, and two cases (NP is covered or not by the grafted polymer chains) as they appear in different melts for different parameters, as indicated. The rest of the figure illustrates examples of mixed (disorder) and demixed (order) melts for different sets of parameters as indicated. D is the size of the core NP, N_g is the number of grafted chains, N is the length of each tethered polymer chain, and ϵ_{AB} expresses the incompatibility between red and blue beads (smaller values of ϵ_{AB} correspond to larger incompatibility). The temperature for all systems was $T = 0.8\epsilon/k_B$.

due to the small size of the core NP. A previous study¹² has determined that the possible maximum number of grafted chains for the $D = 1\sigma$ case is $N_g = 16$. Moreover, grafted polymer chains are homogeneously distributed on the NP's surface by using the Fibonacci lattice (Fig. 1, upper left panel). The length of the polymer chains is N , which ranges from 5 to 40. Thus, our melts are symmetric in architecture and composition, namely each NP has the same number of polymer chains with the same length, while half of these PGNPs have type A grafted polymer chains and the other half has NPs with tethered polymers of type B. Beads of type c, A, and B interact by means of the Lennard-Jones (LJ) potential

$$U_{LJ} = 4\epsilon_{ij} \left[\left(\frac{\sigma_{ij}}{r} \right)^{12} - \left(\frac{\sigma_{ij}}{r} \right)^6 \right], \quad (1)$$

where r_{ij} is the distance between any beads of type i and j . The potential is cut and shifted with the cutoff distance for the interactions between polymer beads being $r_c = 2.5\sigma_{ij}$. The cutoff distance between any pair of interactions that involve the core particle is set to $2^{1/6}\sigma_{ij}$. The potential parameters in our case are $\sigma_{AA} = \sigma_{BB} = \sigma_{AB} = \sigma$ and $\epsilon_{AA} = \epsilon_{BB} = \epsilon$. In our study, the size of the spherical NPs varied, namely we explored the cases $D = \sigma_{cc} = \sigma, 4\sigma$ and 7σ . Also, the cross-interaction ϵ_{AB} between A and B beads, which is used to cross the order-disorder transition, typically varied between 0.5ϵ and 1.0ϵ . Hence, the degree of incompatibility between type A and B polymer chains is introduced by varying ϵ_{AB} ²⁹. Polymer chains are fully flexible and they are connected by harmonic bonds, namely $V_h = k(r - r_0)^2$, where $r_0 = \sigma$ is the equilibrium bond length and $k = 10000\epsilon/\sigma^2$ is a constant. Grafted beads are immobile on the surface of the core NP. Depending on the particular parameters, we run our simulations up to 10^9 MD time steps, with each time step corresponding

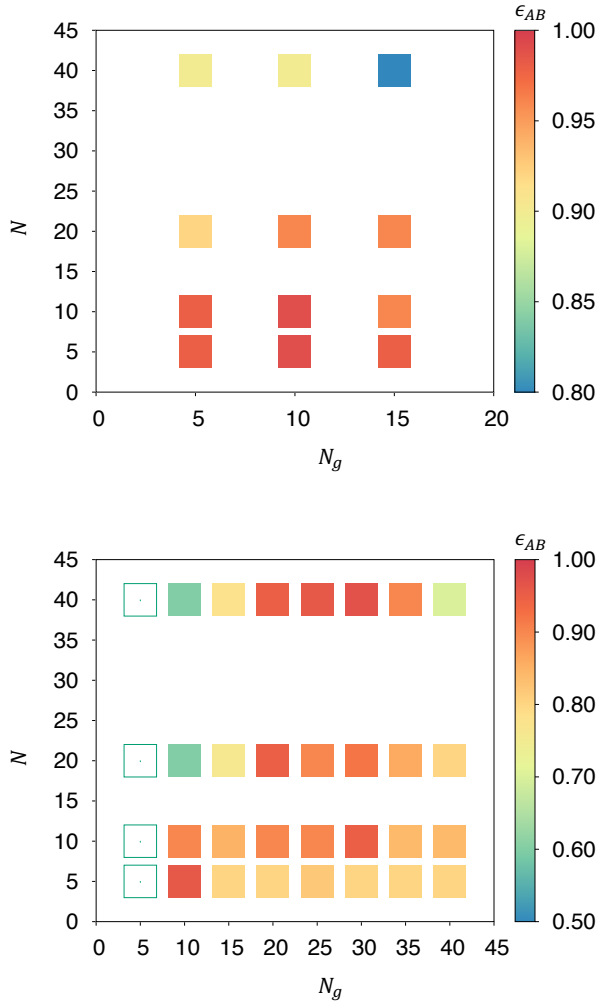


Fig. 2 Phase diagrams of PGPNs for the case $D = 1\sigma$ (star polymers, upper panel) and $D = 4\sigma$ (lower panel) as a function of the chain length, N , and the number of grafted chains, N_g . Open squares indicate a disordered phase for all ϵ_{AB} values explored in this work. The colour bar denotes the ODT by means of the potential interaction ϵ_{AB} .

to $\delta t = 0.005\tau$, where $\tau = \sigma(m/\epsilon)^{1/2}$ is the natural time unit with m indicating the unit of mass. Each simulation at a lower ϵ_{AB} is a continuation of a previous simulation at higher ϵ_{AB} . This procedure was employed for different initial snapshots. Moreover, we did not observe any hysteresis effects when we repeatedly increased or decreased the value of ϵ_{AB} close to the demixing point. Given previous studies of these systems that suggest a star-forming liquid behaviour for $D > 5\sigma$ and $N_g > 60$, we can assume that our conclusions are not affected by kinetic limitations in our systems¹².

3 Results and Discussion

Our results obtained by MD simulations are summarised in Fig. 2, where the phase diagrams for two different cases are illustrated ($D = 1\sigma$, upper panel and 4σ , lower panel) as a function of the polymer chain length N and the number of grafted chains N_g . The colour bar indicates the value of the parameter ϵ_{AB} for which

PGPNs with different type of grafted polymer chains can separate adopting morphologies such as the ones shown in Fig. 1. Lower values of ϵ_{AB} indicate higher demixing difficulty, whereas larger values of ϵ_{AB} indicate much easier demixing of the PGPNs. The ϵ_{AB} values of Fig. 2 are reported as Supplementary Information. Figure 1 also illustrates examples of mixed (disordered, middle panel) and demixed (ordered, right panel) states. Therefore, the value of ϵ_{AB} relates to the ODT of our systems. The phase diagram for $D = 7\sigma$ is not presented here, as no phase separation between PGPNs with chains of type A and B could be achieved within the available simulation time for the range of N and N_g values considered, in agreement with previous studies¹². In the case of $D = 7\sigma$, we were able to detect only disordered configurations such as the ones illustrated in Fig. 1 (middle bottom panel). Overall, we have found that the increase of the core particle hinders the phase separation of the systems for given N and N_g . Moreover, our results suggest that there is a threshold for the size of the core particle that prevents demixing of the PGPNs. For a given size of the core particle, the dependence on N_g and N is not trivial (e.g. monotonic), and will be discussed below for two different cases of NP diameter, D , namely for the cases $D = 1\sigma$ and 4σ .

The case $D = 1\sigma$ (Fig. 2, upper panel) indicates that the phase separation takes place easier when the length of the polymer chains is small (e.g., $N = 5$, Fig. 2, upper panel). In this case, values of $\epsilon_{AB} \approx 0.98$ can induce a phase separation between PGPNs with polymer chains of different type. Hence, a very small incompatibility between the different chemical beads of the grafted polymer chains leads to PGPNs segregation. Moreover, differences in the grafted density seem to play a minor role in the ODT for small chain length, N , which indicates that PGPNs behave like small LJ beads with a similar effective diameter for the range of N_g considered here (Fig. 2, upper panel). However, as the chain length, N , increases the dependence on N_g is more pronounced and the resulting behaviour varies, depending on the value of N . For example, in the case of $N = 20$ an increase of the grafting density N_g leads to a much easier demixing, a trend which is opposite for $N = 40$ (Fig. 2, upper panel), which is an effect of the interplay between N_g and N . Any further conclusions at this point in the case of $D = 1\sigma$ would require a much larger range of N_g , which is not possible for $D = 1\sigma$. Therefore, we continue our discussion with the $D = 4\sigma$ case.

In the case of $D = 4\sigma$ (Fig. 2, lower panel), we observe that a smaller number of grafted chains (N_g), which exposes the steric interaction between the core particles (when $D = 7\sigma$, even N_g as large as 40 is not able to cover the NP as is illustrated in the left panel of Fig. 1) and minimises the interaction between the grafted polymer chains of different type, hinders the demixing of PGPNs. For example, PGPNs with $N_g = 5$ and chain lengths as long as $N = 40$ cannot shield the steric interaction between the NP cores (Fig. 2, lower panel). Hence, for $N_g = 5$ no phase separation occurs for any of the N values considered in this study. The most interesting behaviour is observed when we keep N constant and vary N_g as the tethered polymer chains start to occupy the NP's surface with attractive beads. If we consider the case $N = 5$, then $N_g = 10$ indicates easy segregation of the PGPNs (Fig. 2, lower panel). However, further increase of N_g leads to a higher stability

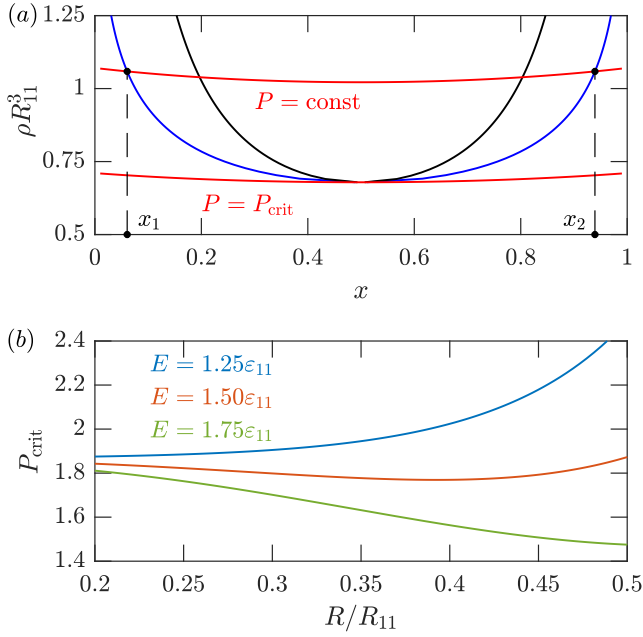


Fig. 3 The effect of growing core on the critical pressure of mixing–demixing transition. (a) Binodal (blue) and spinodal (black) of mixing–demixing transition in the model fluid. The coexisting phases with molar fractions x_1 and x_2 lie at the intersection of the binodal with the isochore $P = \text{const}$ (red). The demixing transition only happens above $P = P_{\text{crit}}$. (b) The dependence of P_{crit} on the radius of the hard-sphere repulsion for different coupling between the hard-sphere and soft repulsion.

of the melt, which seems to be independent of the number of the attached polymer chains. In the latter case, the increase in N_g leads to an increase of the effective steric core interaction of the PGNPs³⁴, which eventually results in more difficult demixing, due to the increase of the effective core size of the PGNPs. In the case of $N = 10$, the change in behaviour with increasing N_g takes place within a broader range of N_g values, due to the higher value of the chain length N . As we increase the chain length N , the dependence on increasing values of N_g is similar (Fig. 2, lower panel). A detailed analysis of our data yields the following key points: On the one hand, the increase of the number of grafted chains, N_g , results initially in better demixing between PGNPs of different type (A- or B-type of polymer chains). On the other hand, further increase of N_g leads to an effective increase in the size of NPs, which in turn hinders the phase separation of the PGNPs. The interplay between these two effects depends on the size of the NPs, D , and the chain length, N , of the grafted polymers. In general, the increase of the chain length favours phase separation, as expected ($\chi_{\text{eff}} \sim N_{\text{eff}}$). These parameters determine the value of ϵ_{AB} where segregation of A- and B-type PGNPs will take place.

We can try to explain the above effect with the help of a simple mean-field model, which coarse-grains the complicated interactions between PGNPs in the melt. As prompted, e.g. by the first column of Fig. 1, the increase of the polymer chain lengths leads to the effective coating of the PGNP actual core particle in the melt, to the point where the entire melt can be approximated as being made up from effective ‘particles’ with larger cores of different sizes and rigidity. These effective ‘particles’ represent our level

of coarse-graining. Still, the interactions between PGNPs are too complex, because the cores depend non-trivially on the grafting densities and chain lengths, and we would like to introduce further simplifications by splitting the interaction into simple parts:

$$\varphi_{ij}^{\text{total}}(r) = \varphi_{ij}^{\text{pol}}(r) + \varphi^{\text{hs}}(r) + \varphi_{ij}^{\text{soft}}(r), \quad (2)$$

where i and j index the polymer species. Since each PGNP is formed by grafting a hard particle with softly repulsive polymer chains, our effective interaction must include the potential of polymer chains. Such soft inter-chain repulsions are usually modelled by the generalized Gaussian-core potential:^{35,36}

$$\varphi_{ij}^{\text{pol}}(r) = \epsilon_{ij} \exp(-r^2/R_{ij}^2). \quad (3)$$

In polymer mixtures, R_{ij} correspond to the gyration radii of the components (with $R_{12} = \sqrt{(R_{11}^2 + R_{22}^2)/2}$), and ϵ_{ij} models the repulsion strength. In our case, the chains are attached to the PGNP core particle, but the chain-induced interactions must be present in the model. Therefore, we still associate R_{ij} with the chain length (N), but the strength of interaction should obviously be related to the number of chains, attached to the same PGNP core (N_g). The next component of the coarse-grained interactions is hard repulsion, caused by the tight wrapping of the polymer chains around the PGNP core. We will model it as a hard sphere of some radius R (where $R \geq D/2$), noting that it is reasonable to expect that higher grafting densities should lead to larger values of R :

$$\varphi^{\text{hs}}(r) = \begin{cases} 0, & \text{if } r > R \\ \infty, & \text{if } r \leq R. \end{cases} \quad (4)$$

Lastly, we need to account for the soft interactions, just outside of the hard core. These are caused by the “loose” parts of the wrapped polymer chains. For simplicity, we use the same form of the soft potential as we did for the free chains:

$$\varphi_{ij}^{\text{soft}}(r) = E_{ij} \exp(-r^2/R^2). \quad (5)$$

The resulting bulk free energy per particle of the mixture as a function of the molar fraction x and total density ρ is given by the following expression

$$f(x, \rho) = f_{\text{id}}(x, \rho) + f_{\text{hs}}(x, \rho) + f_{\text{mf}}(x, \rho), \quad (6)$$

where the ideal part $f_{\text{id}}(x, \rho)$ is defined as

$$f_{\text{id}}(x, \rho) = k_B T (x \log x + (1-x) \log (1-x) + \log \rho - 1), \quad (7)$$

the hard-sphere part is modelled using the Percus–Yevick equation of state, which in our case is independent of x , due to symmetry

$$f_{\text{hs}}(x, \rho) = k_B T \left(\frac{3(2-\eta)\eta}{2(1-\eta)^2} - \log(1-\eta) \right), \quad \eta = \frac{4}{3} \pi R^3 \rho, \quad (8)$$

and the soft repulsive part due to $\varphi_{ij}^{\text{pol}}(r) + \varphi_{ij}^{\text{soft}}(r)$ is given by the mean-field term³⁶

$$f_{\text{mf}}(x, \rho) = \frac{1}{2} \rho \left((1-x)^2 V_{11} + 2x(1-x) V_{12} + x^2 V_{22} \right), \quad (9)$$

with V_{ij} being the total integrated strength of the potential:

$$V_{ij} = \pi^{3/2} (R_{ij}^3 \varepsilon_{ij} + R^3 E_{ij}), \quad (10)$$

where due to symmetry we can set $E_{11} = E_{22} = 1$, leaving us with $E_{12} = E$ as the coupling parameter. The mean-field treatment we follow supposes that the hard-sphere particles are moving in a uniform repulsive field induced by the soft potential $\varphi_{ij}^{pol}(r) + \varphi_{ij}^{soft}(r)$. This approach is essentially the same as the one which underpins the celebrated van der Waals equation of state of simple liquids,³⁷ with a change that the perturbation in our case is given by soft repulsions.^{35,36} We further chose a system of units where $R_{11} = R_{22} = 1$ and $\varepsilon_{11} = \varepsilon_{22} = 1$. To ensure phase separation at small values of R , we fix $\varepsilon_{12} = 1.2\varepsilon_{11}$, and in order to enhance the effects even further we set $T = 0.4\varepsilon_{11}$.

The picture of phase coexistence is summarised in Fig. 3(a). Here the densities and molar fractions of the coexisting demixed phases are found as the intersections of the binodal curve (blue) with the isochores $\rho(x)$: $P = \text{const}$ (red). The mixing/demixing transition is accessible above the critical pressure P_{crit} . In addition, we show the boundaries of stability of the demixed phases – the spinodal (black curve). A qualitative agreement with the results in Fig. 2 is expressed by the dependence of the critical pressure on the hard core radius R , plotted in Fig. 3(b) for several values of the coupling parameter. There are three possible scenarios which $P_{\text{crit}}(R)$ may follow. For weak and strong coupling ($E = 1.25$ and $E = 1.75$), the dependence of $P_{\text{crit}}(R)$, is monotonic. This means that increasing N_g should make the transition respectively less and more accessible. Notice the existence of the intermediate regime at $E = 1.50$, where $P_{\text{crit}}(R)$ has a local minimum. In this case, increasing N_g should initially facilitate phase separation (by reducing $P_{\text{crit}}(R)$), but further increase of N_g should actually inhibit phase separation, as P_{crit} starts to grow.

We have also analysed various structural properties from MD simulations that contain information on the interplay between the growing with N_g effective core size and the growing with N effective chain length of the polymers. All our results are for the case $\epsilon_{AB} = 1.0$ in order to isolate the structural components that may play a role in the phase separation of PGNPs. Figure 4(a) presents results for the end-to-end distance of the polymer chains, *i.e.*, the distance between the bead attached onto the core NP and the free end of each polymer chain, $\langle R_{ce}^2 \rangle^{1/2}$. An average over all chains for each PGNP and an ensemble average is taken. Results for the most interesting case $D = 4\sigma$ are presented in Fig. 4(a), where more data is also available as a wider range of N_g is possible. Our results suggest a trend that the chain size is larger in the case of systems that undergo easier demixing (e.g. $N_g > 15$), which may suggest that grafted polymer chains be closer to the NPs and the core effect be more pronounced. Moreover, an increase in the average number of neighbours (Fig. 4(b)), $\langle \bar{M}_{AB} \rangle$, is observed for small values of N_g , which may indicate a larger role of the effective core interactions in this case, in agreement with the trend observed in the case of $\langle R_{ce}^2 \rangle^{1/2}$. In particular, $\langle \bar{M}_{AB} \rangle$ overall decreases for each N when N_g increases, but a peak appears for small N_g . This peak disappears when the number of grafted chains $N_g > 15$. Here, PGNPs are considered as neighbours

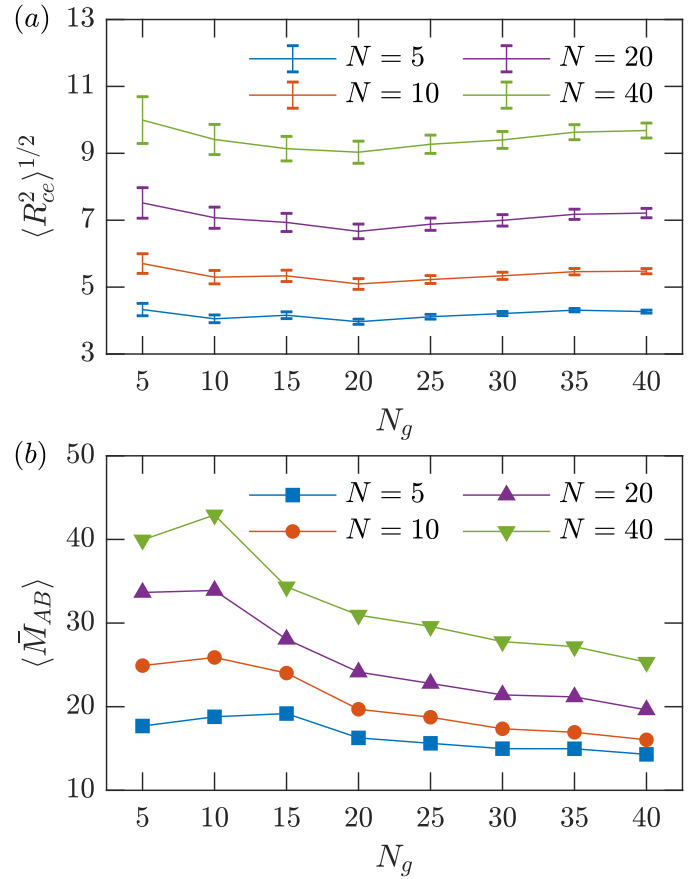


Fig. 4 For the case $D = 4\sigma$ and different chain lengths N , we plot as functions of N_g : (a) End-to-end distance of grafted chains (with error bars), and (b) Average number of neighbours for each PGNP.

when at least one of the beads belonging to different PGNPs interact without attempting to analyse possible differences in the morphologies of polymer chains that may depend on the relative position/orientation of neighbouring PGNPs^{38,39}. The analysis of the average number of neighbours based only on the colloids (ignoring the polymer chains) did not show any sensitivity on the variation with N_g . Overall, $\langle R_{ce}^2 \rangle^{1/2}$ and $\langle \bar{M}_{AB} \rangle$ show some correlation with the phase behaviour of Fig. 2, but a direct correlation of both properties with the phase diagram should not be overstated. In general, we observe a larger variation of $\langle R_{ce}^2 \rangle^{1/2}$ with N_g for larger values of N and smaller chain dimensions for smaller N_g values. The smaller $\langle R_{ce}^2 \rangle^{1/2}$ combined with the increase in $\langle \bar{M}_{AB} \rangle$ for $N_g < 20$ may suggest an increased influence of the effective core size of the PGNPs.

4 Concluding Remarks

We have studied the mixing–demixing behaviour of molecularly and compositionally symmetric melts with spherical NPs with different chemical types of grafted chains by using MD simulations of a coarse-grained model. The size of the NP, the number of grafted chains, and the length of the side chains were varied in order to investigate the phase behaviour of these systems. Our results indicate that the increase of the NP size hinders the

phase separation. Moreover, the system cannot separate beyond a certain NP size for given grafting density and length of polymer chains. The phase behaviour of intermediate NP sizes (*i.e.*, $D = 4\sigma$) indicates a transition region as the grafting density increases and the steric repulsions are occupied by an attractive core with larger effective diameter, which is formed by the tethered polymer chains. We have explained these effects and provided an analytical description by means of a mean-field theory model. We anticipate that our results will provide further insight into the phase behaviour of PGNPs, guided by the interplay phenomena between the NP size, the chain length, and the grafting density as illustrated in this work, with implications in materials science and medicine.

Conflicts of interest

There are no conflicts to declare.

Acknowledgements

The authors acknowledge useful discussions with Alexandros Chremos. This research was supported in part by PLGrid Infrastructure.

Notes and references

- 1 A. Balazs, T. Emrick and T. Russell, *Science*, 2006, **314**, 1107–1110.
- 2 S. Choudhury, A. Agrawal, S. A. Kim and L. A. Archer, *Langmuir*, 2015, **31**, 3222–3231.
- 3 J. L. Schaefer, S. S. Moganty, D. A. Yanga and L. A. Archer, *J. Mater. Chem.*, 2011, **21**, 10094–10102.
- 4 J. B. Hooper and K. S. Schweizer, *Macromolecules*, 2005, **38**, 8858–8869.
- 5 J. B. Hooper and K. S. Schweizer, *Macromolecules*, 2006, **39**, 5133–5142.
- 6 D. Sunday, J. Ilavsky and D. L. Green, *Macromolecules*, 2012, **45**, 4007–4011.
- 7 S. Srivastava, S. Choudhury, A. Agrawal and L. A. Archer, *Curr. Opin. Chem. Eng.*, 2017, **16**, 92–101.
- 8 S. Srivastava, J. Schaefer, Z. Yang, Z. Tu and L. Archer, *Adv. Mater.*, 2014, **15**, 201–234.
- 9 R. Mangal, S. Srivastava and L. Archer, *Nat. Commun.*, 2015, **6**, 7198.
- 10 S. Srivastava, P. Agarwal and L. Archer, *Langmuir*, 2012, **28**, 6272–6281.
- 11 A. Agrawal, B. M. Wenning, S. Choudhury and L. A. Archer, *Langmuir*, 2016, **32**, 8698–8708.
- 12 A. Chremos and A. Z. Panagiotopoulos, *Phys. Rev. Lett.*, 2011, **107**, 105503.
- 13 A. Chremos, A. Z. Panagiotopoulos, H. Y. Yu and D. L. Koch, *J. Chem. Phys.*, 2011, **135**, 114901.
- 14 A. Chremos and J. F. Douglas, *Soft Matter*, 2016, **12**, 9527–9537.
- 15 A. Chremos and J. F. Douglas, *Ann. Phys.*, 2017, **529**, 1600342.
- 16 H.-Y. Yu and D. L. Koch, *Langmuir*, 2010, **26**, 16801–16811.
- 17 H.-Y. Yu, S. Srivastava, L. A. Archer and D. L. Koch, *Soft Matter*, 2014, **10**, 9120–9135.
- 18 P. Agarwal, H. Qi and L. A. Archer, *Nano Lett.*, 2010, **10**, 111–115.
- 19 N. J. Fernandes, H. Koerner, E. P. Giannelis and R. A. Vaia, *MRS Commun.*, 2013, **3**, 13–29.
- 20 A. Agrawal, H.-Y. Yu, S. Srivastava, S. Choudhury, S. Narayanan and L. A. Archer, *Soft Matter*, 2015, **11**, 5224–5234.
- 21 S. A. Kim, R. Mangal and L. A. Archer, *Macromolecules*, 2015, **48**, 6280–6293.
- 22 P. Agarwal, S. A. Kim and L. A. Archer, *Phys. Rev. Lett.*, 2012, **109**, 258301.
- 23 S. A. Kim and L. A. Archer, *Macromolecules*, 2014, **47**, 687–694.
- 24 S. Choudhury, R. Mangal, A. Agrawal and L. A. Archer, *Nat. Commun.*, 2015, **6**, 10101.
- 25 S. Goyal and F. A. Escobedo, *J. Chem. Phys.*, 2011, **135**, 184902.
- 26 P. Agarwal, S. Srivastava and L. A. Archer, *Phys. Rev. Lett.*, 2011, **107**, 268302.
- 27 K. Meyer, *Helv. Chim. Acta*, 1940, **23**, 1063–1070.
- 28 P. J. Flory, *Principles of Polymer Chemistry*, Cornell University Press, Ithaca, NY, 1953.
- 29 A. Chremos, A. Nikoubashman and A. Z. Panagiotopoulos, *J. Chem. Phys.*, 2014, **140**, 054909.
- 30 K. Kremer and G. S. Grest, *J. Chem. Phys.*, 1990, **92**, 5057.
- 31 A. Chremos and P. E. Theodorakis, *ACS Macro Lett.*, 2014, **3**, 1096–1100.
- 32 A. Chremos and P. E. Theodorakis, *Polymer*, 2016, **97**, 191–195.
- 33 S. J. Plimpton, *J. Comput. Phys.*, 1995, **117**, 1–19.
- 34 A. Chremos and J. F. Douglas, *J. Chem. Phys.*, 2015, **143**, 111104.
- 35 A. A. Louis, P. Bolhuis and J. P. Hansen, *Phys. Rev. E*, 2000, **62**, 7961.
- 36 A. Archer and R. Evans, *Phys. Rev. E*, 2001, **64**, 041501.
- 37 J. Hansen and I. McDonald, *Theory of Simple Liquids (3rd edn)*, Elsevier, 2006.
- 38 A. Travesset, *ACS Nano*, 2017, **11**, 5375–5382.
- 39 C. Waltmann, N. Horst and A. Travesset, *ACS Nano*, 2017, **11**, 11273–11282.